MOLECULAR AND CELLULAR BIOLOGY, May 1994, p. 3030–3040
0270-7306/94/$04.00+0

Vol. 14, No. 5

Nuclear Localization and Cell Cycle Regulation of a Murine Protein Tyrosine Phosphatase

ULRICH TILLMANN,[1] JOHN WAGNER,[2] DEREK BOERBOOM,[2] HEINER WESTPHAL,[1] AND MICHEL L. TREMBLAY[2]*

Laboratory of Mammalian Genes and Development, National Institute of Child Health and Human Development, Bethesda, Maryland 20892,[1] and Department of Biochemistry, McGill University, Montreal, Quebec, Canada H3G 1Y6[2]

Received 22 December 1993/Accepted 7 February 1994

MPTP is a murine homolog of the human T-cell protein tyrosine phosphatase (PTPase) and the rat PTP-S enzyme. Enzymatic activity of this ubiquitously expressed protein was demonstrated in immunoprecipitates from NIH 3T3 cells and in recombinant protein overexpressed in bacteria. Expression of β-galactosidase–MPTP chimeric proteins in COS1 cells identified a nuclear localization signal at the carboxyl terminus of the MPTP that was sufficient to direct β-galactosidase as well as a tagged version of the MPTP to the nucleus. Deletion analysis of amino acids within the nuclear targeting signal showed that this sequence does not conform to the bipartite type of nuclear localization signals. Furthermore, it was shown that the steady-state levels of MPTP RNA fluctuate in a cell cycle-specific manner. On the basis of these experiments, we discuss the possible function of MPTP in the cell cycle and other nuclear processes.

In the past decade, an enormous amount of information has been gathered on the multifaceted involvement of protein phosphorylation in biology. Tyrosine phosphorylation has drawn special attention because of its role in key processes such as signal transduction, cellular differentiation, and cell cycle progression. Through these processes, it has been shown to influence growth, development, and oncogenic transformation. The level of tyrosine phosphorylation results from the activity of both tyrosine-specific kinases and phosphatases. The importance of protein tyrosine phosphatases (PTPases) has been recognized more recently by the cloning and characterization of an ever-growing number of these genes. Structurally, the PTPase family can be subdivided into two groups: receptor-like PTPases and intracellular enzymes (9). With some exceptions, the receptor-like enzymes feature large and diverse extracellular domains and two tandemly arranged intracellular PTPase conserved domains. Much like their receptor phosphotyrosine kinase counterparts, most bind as yet undefined ligands at their extracellular domains. The cloning of intracellular PTPases that possess SH2 domains provides a clue about the molecular function of at least a small subset of these polypeptides (27). For example, the SH2-containing PTPase *corkscrew* is involved in a signal transduction pathway responsible for cell fate at the termini of *Drosophila* embryos (22).

A prototype of the intracellular PTPases is the well studied T-cell PTPase (6). Although isolated from a human T-cell cDNA library, this enzyme is ubiquitously expressed in human tissues. In vitro expression of the cDNA yields an inactive enzyme that can be activated by trypsin cleavage of a hydrophobic carboxyl terminus (37). This stretch of hydrophobic amino acids is thought to anchor the enzyme to high-molecular-weight complexes from which it can be released and activated by proteolytic processing.

In a previous study, we isolated the murine homolog of the T-cell PTPase, termed MPTP, that is expressed in all tissues and stages of development (20). The MPTP amino acid sequence is 93.2% identical to that of the human T-cell PTPase. The major sequence divergence occurs at the carboxyl terminus, where the mouse enzyme lacks the unique hydrophobic domain. The same holds true for the rat enzyme PTP-S (33). To clarify the obvious discrepancy between the rodent and human enzymes, we and others cloned a human message that encodes a T-cell PTPase with a carboxyl terminus identical to that of MPTP (2, 20). Since this novel message was found to be the most abundant transcript in a variety of human tissues (20), we distinguished them as T-cell PTPa (identical to MPTP) and T-cell PTPb (containing the hydrophobic carboxyl terminus) (see Fig. 8).

All human and rodent forms of T-cell PTPase also contain a putative bipartite nuclear targeting motif at their carboxyl termini. With some exceptions such as *Drosophila* dPTP61F (19), only one major group of PTPases, the *cdc25* gene product and its various homologs, has so far been found to localize to the nucleus. These enzymes play a critical role in the eukaryotic cell cycle (1, 8, 11). A possible involvement for the T-cell PTPase in the cell cycle was proposed on the basis of the findings that this enzyme successfully utilizes the yeast *cdc2* kinase as a substrate in vitro and that it can complement an inactive yeast *cdc25* PTPase mutant in vivo (12). In addition, overexpression of a truncated T-cell PTPase in BHK cells results in a 50% decrease in the mitotic index (5), caused by cytokinetic failure and asynchronous cellular division (4). Similarly, this truncated T-cell PTPase causes the suppression of v-*fms*-induced transformation in Rat-2 cells (36).

The important regulatory function attributed to the hydrophobic carboxyl terminus of T-cell PTPb and its absence in the most abundant T-cell PTPase transcripts of humans, rats, and mice prompted us to characterize the enzymatic properties of a full-length MPTP protein. Furthermore, because of the possible involvement of the T-cell PTPase enzymes (and by analogy the MPTP) in the cell cycle, we evaluated the potential

* Corresponding author. Mailing address: Department of Biochemistry, McIntyre Medical Sciences Building, McGill University, Montreal, Quebec, Canada H3G 1Y6. Phone: (514) 398-7290. Fax: (514) 398-7384. Electronic mail address: tremblay@medcor.mcgill.ca.

nuclear targeting properties of the carboxyl terminus and the MPTP mRNA levels throughout the cell cycle.

MATERIALS AND METHODS

Enzymes and reagents. Restriction and modifying enzymes were purchased from Boehringer Mannheim and used as instructed by the manufacturer. Peptides P1 (NH_2-K-V-H-C-S-A-G-V-G-R-T-G-COOH) and P2 (NH_2-K-R-K-R-P-R-L-T-D-T-COOH) were from Synthecell Corp. Other chemicals were purchased from Sigma.

PCR amplification of the MPTP coding region. MPTP cDNA in pBluescript SK (Stratagene) served as a template in the PCR amplification of various parts of the protein coding region, using the following oligonucleotide primers: MPTP oligonucleotide 29 (5′-GGG GGA TCC ATG TCG GCA ACC ATC GAG CGG G-3′); MPTP oligonucleotide 14 (5′-CCC GGG AAT TCT CAT TAG GTG TCT GTC AAT CTT GGC CTT-3′); MPTP oligonucleotide 21 (5′-CCC GGG ATC CCC GGA CCA ACT CAG ATT CTC CTA CAT GGC C-3′); MPTP oligonucleotide 38 (5′-CCG GCG GCC TCA TTA GGT GTC TGT CAA TCT TGG CCT T-3′); MPTP oligonucleotide 41 (5′-CCC GTC GAC CCG GAC CAA CTC AGA TTC TCC TAC ATG GCC-3′); MPTP oligonucleotide 43 (5′-CCG GCG GCC GCC TCA TTA TTC ATT TAG CCT CTG TTT CAT CTG CTG GAC C-3′); MPTP oligonucleotide 44 (5′-CCG GCG GCC GCC AAG CTT TCA TTA GGT GTC TGT CAA TCT TGG CCT T-3′); MPTP oligonucleotide 45 (5′-CGG CGT CGA CAG AAA GGC TAC GAC GGC TCA GAA GGT GC-3′); and MPTP oligonucleotide 46 (5′-CGG CGT CGA CCG GAA ACG TAT TCG AGA GGA TAG AAA GGC-3′).

PCRs were performed with 0.4 μg of each oligonucleotide through 25 cycles of 90 s at 94°C and 150 s at 72°C in a Perkin-Elmer Cetus PCR cycler.

Construction of bacterial expression vectors. For the generation of a full-length glutathione *S*-transferase (GST)–MPTP fusion protein (Fig. 1A), a portion of the MPTP cDNA (nucleotides 67 to 1215) was amplified with MPTP oligonucleotides 29 and 14 such that *Bam*HI and *Eco*RI restriction sites were introduced at the 5′ and 3′ ends, respectively. In the process, a dipeptide linker (Gly-Ser) was inserted between the GST and MPTP protein moieties. The dipeptide remains attached to the MPTP after enzymatic cleavage of the fusion protein with thrombin.

The fusion between GST and the C-terminal 120 amino acids of the MPTP (pGEX-MPTP-C120) (Fig. 1A) was achieved by amplification of a DNA segment spanning nucleotides 850 to 1215 with MPTP oligonucleotides 21 and 14, thereby introducing *Bam*HI and *Eco*RI restriction sites as described above. After digestion with *Eco*RI and *Bam*HI, the PCR products were reisolated from an agarose gel and cloned in frame with GST in the bacterial expression vector pGEX-2T (Pharmacia).

Bacterial expression and purification of GST fusion proteins. *Escherichia coli* DH5α (Bethesda Research Laboratories) transformed with the pGEX plasmids was grown in LB to an A_{600} of 1.0 and induced with 1 mM isopropyl-β-D-thiogalactopyranoside (IPTG) (Boehringer Mannheim) for 3 h. GST fusion proteins were isolated as described by Smith and Johnson (31). The proteolytic cleavage of the fusion proteins was performed after immobilization on glutathione-Sepharose and overnight incubation with 4 U of thrombin (Boehringer Mannheim) at room temperature.

Eukaryotic expression constructs. For expression of a truncated MPTP gene as a fusion with *lacZ* (Fig. 1B), the eukaryotic expression vector pCH110 (Clontech) was modified as follows. The plasmid was partially digested with *Eco*RI, the linearized vector was recovered from an agarose gel, and the overhangs were blunt ended with deoxyribonucleotides and the Klenow fragment of DNA polymerase I. After religation and transformation into bacteria, a plasmid, pCH110ΔR1, that retained only the *Eco*RI site at the 3′ end of the *lacZ* gene was identified. The complementary oligonucleotides *lacZ* C18T (5′-AAT TTC AGC TGA GCG CCG GTC GCT ACC ATT ACC AGT TGG TCT GGT GTG TCG ACT AAG CGG CCG C-3′) and *lacZ* C18B (5′-AAT TGC GGC CGC TTA GTC GAC ACA CCA GAC CAA CTG GTA ATG GTA GCG ACC GGC GCT CAG CTG A-3′) were annealed, and the double-stranded fragment was cloned into pCH110ΔR1 that had been linearized with *Eco*RI. The resulting plasmid, pCH110.1, has a reduplication of the sequences encoding the last 18 amino acids of β-galactosidase with an in-frame *Sal*I site 5′ of the termination codon followed by a *Not*I restriction site.

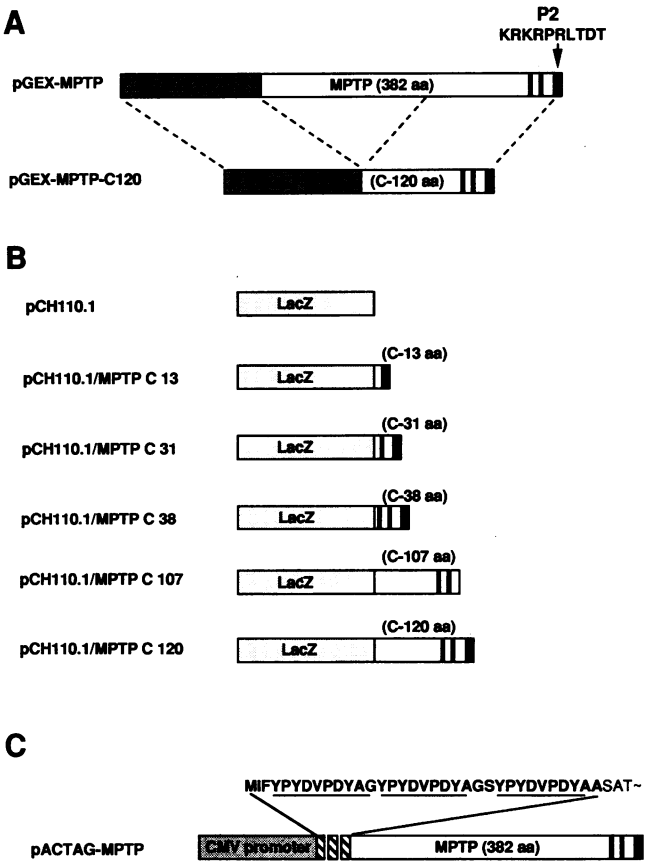

FIG. 1. Schematic representation of fusion protein constructs. (A) Fusion proteins from plasmids pGEX-MPTP and pGEX-MPTP-C120. The shaded area represents the GST coding sequence; the open area indicates the MPTP coding sequence. The position and sequence of peptide P2 are marked by the black region. aa, amino acids. (B) pCH110.1/MPTP plasmids. Shaded regions represent the *lacZ* coding sequences; open areas indicate the various MPTP coding sequences used in the fusion proteins. (C) Structure of pACTAG-MPTP. The shaded area indicates the cytomegalovirus (CMV) promoter sequence. The striped region represents the three HA epitope motifs recognized by antibody 12CA5. The amino acid sequence of the epitope is underlined above. The open area encodes the full-length MPTP protein. Vertical bars designate basic amino acid clusters.

Sequences encoding the C-terminal 107 (nucleotides 850 to 1173), 120 (nucleotides 850 to 1215), 38 (nucleotides 1098 to 1215), and 31 (nucleotides 1119 to 1215) amino acids of the MPTP were amplified by using MPTP oligonucleotides 41 and 43, MPTP oligonucleotides 41 and 38, MPTP oligonucleotides 44 and 46, and MPTP oligonucleotides 44 and 45, respectively. After gel purification, the products were digested with *Sal*I and *Not*I, reisolated from an agarose gel, and cloned into *Sal*I- and *Not*I-digested pCH110.1. The resulting plasmids were designated pCH110.1/MPTP-C107, pCH110.1/MPTP-C120, pCH110.1/MPTP-C38, and pCH110.1/MPTP-C31, respectively. Finally, the sequences encoding the 13 C-terminal amino acids of the MPTP (nucleotides 1173 to 1215), obtained by annealing the complementary MPTP oligonucleotides C13T (5′-TCG ACA CTG AAC GAA AAA GAA AAA GGC CAA GAT TGA CAG ACA CCT AAA AGC TTG C-3′) and MPTP C13B (5′-GGC CGC AAG CTT TTA GGT GTC TGT CAA TCT TGG CCT TTT TCT TTT TCG TTC AGT G-3′), were cloned by the procedure described above to generate plasmid pCH110.1/MPTP-C13.

Construction of the MPTP-hemagglutinin (HA) tag vector was performed by linearizing the eukaryotic expression vector pACTAG (generated by Alain Charest, McGill University) with *Not*I and retrieving the entire MPTP coding sequence from plasmid pGEX-MPTP with the restriction enzymes *Bam*HI and *Eco*RI. The linearized DNA fragments were isolated from an agarose gel and blunt ended with deoxyribonucleotides and the Klenow fragment of DNA polymerase I. After ligation and transformation, we identified the desired plasmid, pACTAG-MPTP (Fig. 1C), which encoded the MPTP enzyme linked at its amino terminus to three copies of an influenza virus HA epitope that is specifically recognized by monoclonal antibody 12CA5 (21).

Cell culture, transfection, metabolic labeling, and immunoprecipitation. NIH 3T3 cells were grown in Dulbecco modified Eagle medium (DMEM) supplemented with 10% fetal calf serum, 100 U of penicillin per ml, and 100 μg of streptomycin per ml. COS1 cells were grown in the same medium, harvested in the logarithmic growth phase, and washed twice with phosphate-buffered saline (PBS) before transfection by calcium phosphate precipitation (13). For metabolic labeling, 2×10^7 cells were starved for 30 min in DMEM without methionine and serum and then incubated for 2 h with 250 μCi of [^{35}S]methionine in the same medium. Cells were washed two times in cold PBS and then lysed in cold immunoprecipitation buffer containing 50 mM Tris (pH 7.2), 150 mM NaCl, 1% Triton X-100, and 100 kallikrein inhibitor units (KIU) of aprotinin per ml. The cell lysate was incubated on ice for 10 min and then cleared by centrifugation (12,500 × *g* for 20 min at 4°C). To aliquots of the supernatant (10^6 cells per equivalent), appropriate amounts of either affinity-purified immunoglobulin G (IgG) or crude serum and 250 μl of a 10% slurry of protein A-Sepharose in immunoprecipitation buffer were added. For immunocompetition experiments, free peptide (100 ng) or fusion protein (GST–MPTP-C120, 1 μg) was included in the assays. After incubation (4 h, 4°C), the Sepharose beads were collected by low-speed centrifugation, washed four times with ice-cold immunoprecipitation buffer, and then washed twice in phosphatase assay buffer containing 25 mM imidazole (pH 7.3), 1 mM EDTA, 0.1% 2-mercaptoethanol, 2 mM $MgCl_2$, 1 μg of leupeptin, and 250 mM sucrose.

Indirect immunofluorescence microscopy. Immunofluorescence staining of transiently transfected COS1 cells was performed by the method of Lejbkowicz et al. (17), using either a commercially available mouse monoclonal antibody against β-galactosidase (Boehringer Mannheim) or monoclonal antibody 12CA5 directed against the HA epitope (21). Mouse monoclonal antibodies were visualized by using a rhodamine-conjugated goat anti-mouse IgG (Boehringer Mannheim). All photographs were taken at a magnification of ×400.

Polyclonal antibodies and affinity purification. Antisera directed against the purified GST–MPTP-C120 fusion protein or against the carboxyl-terminal peptide P2 cross-linked to hemocyanin (Calbiochem) were generated as follows. Female New Zealand White rabbits were immunized with 250 μg of either antigen in complete Freund's adjuvant by multiple subcutaneous injections. For booster injections at 3-week intervals, 100 μg of the antigen in incomplete Freund's adjuvant was administered in the same manner. Recombinant MPTP (500 μg), obtained by cleaving the GST-MPTP fusion protein with thrombin, was immobilized on Affi-Gel 15 (Bio-Rad) (0.5-ml bed volume) as instructed by the manufacturer. Crude antiserum was diluted (1:10) in PBS and passed over the column three times. After extensive washing with PBS, the specifically bound antibodies were eluted in 0.1 M glycine (pH 3.0), neutralized with 1.0 M Tris (pH 8.0), and transferred into PBS by column buffer exchange. IgG from the preimmune serum of the same animals was purified on protein A-Sepharose (Pharmacia), using the conditions described above. Protein concentrations were determined by the method of Bradford (1a), using the Bio-Rad protein concentration kit.

Phosphatase assay. Dephosphorylation of *p*-nitrophenylphosphate (pNPP) by the purified recombinant MPTP was assayed under the conditions described by Streuli et al. (32). Reactions were performed in the linear range of the assay with 90 ng of enzyme per ml at 30°C for 10 min; 10 N NaOH was added to a final concentration of 2.0 N to terminate the reactions. Production of *p*-nitrophenol was calculated by using a millimolar extinction coefficient of 17.8.

PTPase assays on immunocomplexes were carried out by the following procedure. To identical amounts of immunoprecipitated protein A beads, 3×10^6 cpm of ^{32}P-labeled Raytide (labeled as specified by the manufacturer [Oncogene Science]) was added, and PTPase activity was initiated at 37°C in the presence or absence of 1 mM sodium orthovanadate. At chosen time points, the reactions were stopped by adding 40 μl of bovine serum albumin (1%) followed by 250 μl of 25% trichloroacetic acid. Samples were incubated on ice for 10 min and then spun at 10,000 × *g* for 20 min. Release of radiolabeled phosphate was determined by scintillation counting.

Analysis of MPTP gene regulation during the cell cycle. NIH 3T3 cells were plated at 80% confluency in 60-mm-diameter dishes and synchronized by cultivating the cells in DMEM containing 0.2% serum for 36 h. Alternatively, cell synchronization was obtained by supplementing normal DMEM for 8 h with 2 mM hydroxyurea (Sigma) or for 12 h with 0.4 μg of nocodazole (ICN) per ml. At time zero, the culture medium was replaced with DMEM containing 15% serum. Total RNA was extracted from each 60-mm-diameter dish at 3-h intervals, using an RNA isolation kit (Stratagene). Fifteen micrograms of total RNA was transferred onto a nitrocellulose membrane by using a slot blot apparatus (Bio-Rad). The filter was hybridized with a probe prepared from the MPTP cDNA and washed as described previously (3). To allow for quantitative evaluation of MPTP RNA levels at different time points, the filter was rehybridized with an actin probe. Slot blot autoradiograms of MPTP and actin RNA were quantitated by laser densitometry (LKB 2202 Ultrascan laser densitometer). The

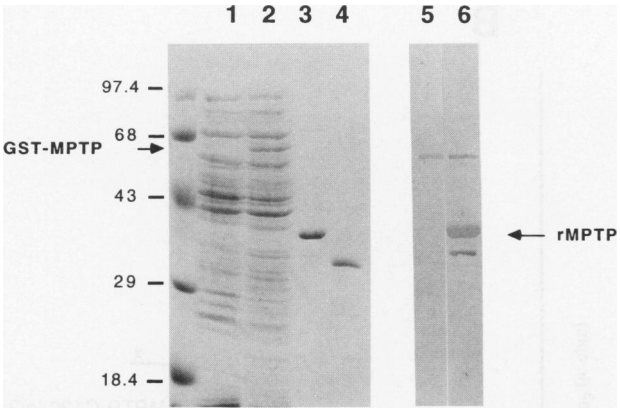

FIG. 2. Bacterial expression of the MPTP. SDS-PAGE (10% gel) of total soluble bacterial proteins and purified recombinant MPTP (rMPTP) is shown. Lanes: 1, total soluble proteins from *E. coli* transformed with pGEX-MPTP without IPTG induction; 2, as lane 1, but after 3 h of IPTG induction; 3, recombinant MPTP enzyme, released from the GST-MPTP fusion protein by thrombin cleavage; 4, GST–MPTP-C120 purified on glutathione-Sepharose; 5 and 6, Western blots of the material in lane 3 with a preimmune IgG (lane 5) and a monospecific IgG directed against the last 10 carboxyl-terminal amino acids of the MPTP. Sizes are indicated in kilodaltons.

MPTP RNA levels were normalized by plotting the ratio of MPTP scanning data against the corresponding actin values.

RESULTS

Bacterial expression of the MPTP. To confirm that the cloned MPTP cDNA encodes an active PTPase, the entire MPTP coding sequence was introduced into the bacterial expression vector pGEX-2T (Fig. 1A). Upon induction by IPTG, bacteria harboring the recombinant plasmid were shown to express a new protein, GST-MPTP, with an apparent molecular mass of approximately 66 kDa (Fig. 2; compare lanes 1 and 2). After adsorption of the fusion protein to glutathione-Sepharose (Pharmacia), the MPTP moiety was released from the column by overnight cleavage with thrombin and eluted. The purified recombinant MPTP (lane 3), like the fusion protein (lane 2), exhibited upon sodium dodecyl sulfate (SDS)-polyacrylamide gel electrophoresis a slightly faster mobility of 40 kDa, versus a theoretical molecular mass of 44 kDa. A similar migration pattern was also observed in the case of the GST-MPTP-C120 fusion protein (lane 4) that was used to raise antibodies against the MPTP. We used these antibodies and an antiserum against an N-terminal peptide of the MPTP to verify that the bacterially expressed product was indeed the MPTP (data not shown). Antiserum 136 raised against peptide P2 representing the last 10 amino acids of the MPTP clearly identified the bacterial product as full-length MPTP on Western blots (immunoblots) (compare lanes 3 and 6). A contaminating band of higher molecular weight was also detected by this antiserum, since it appeared in the preimmune serum (compare lanes 5 and 6). We tested the ability of this recombinant MPTP to function in an in vitro phosphatase assay with pNPP as the substrate. As shown in Fig. 3A, the highly purified full-length recombinant MPTP exhibited significant activity against pNPP. As expected for a PTPase, enzyme activity was severely reduced in a dose-dependent fashion by two potent inhibitors of known PTPases, sodium vanadate and zinc chloride (Fig. 3B). From the Lineweaver-Burk analysis of pNPP dephosphorylation, the recombinant MPTP had a specific

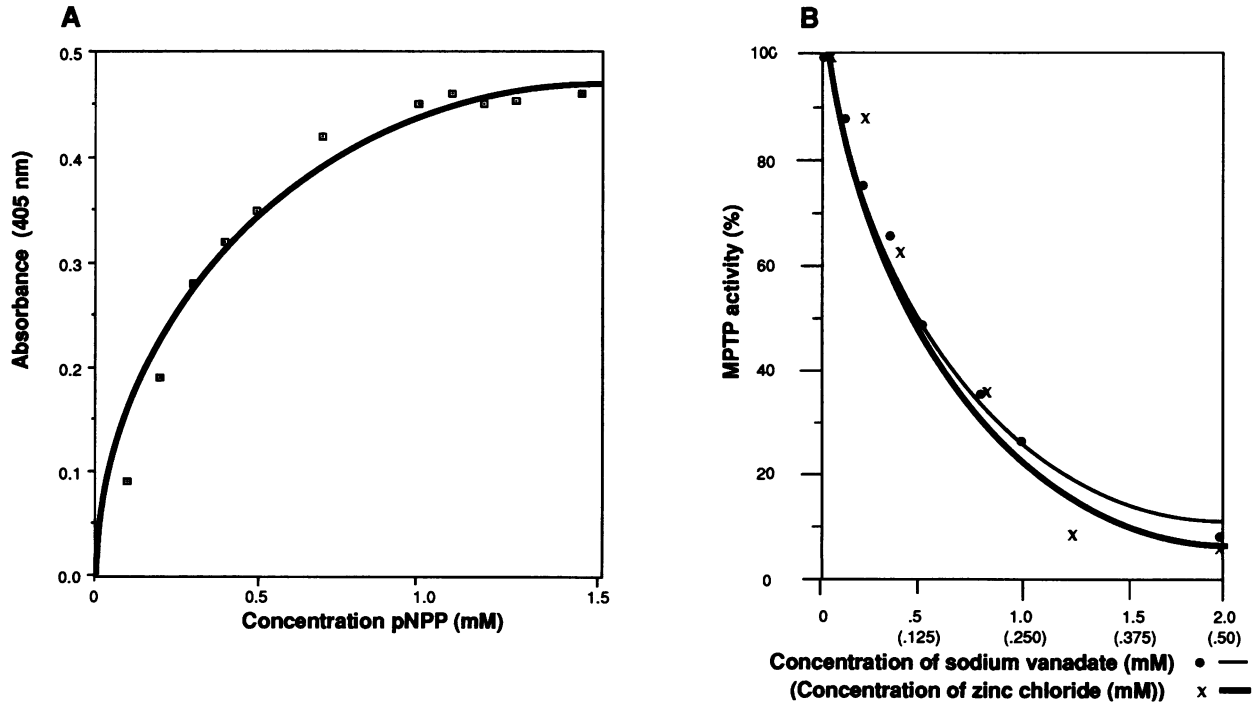

FIG. 3. Phosphatase activity of the MPTP bacterial enzyme, using pNPP as a substrate. Purified recombinant MPTP (90 ng/ml) was assayed in standard phosphatase reaction buffer in the presence of various concentrations of pNPP (A) or of PTPase inhibitors sodium vanadate and zinc chloride (B). The extent of dephosphorylation was assayed by reading the A_{405}. In panel B, values are plotted as decimal fractions of the control activity in the absence of inhibitors.

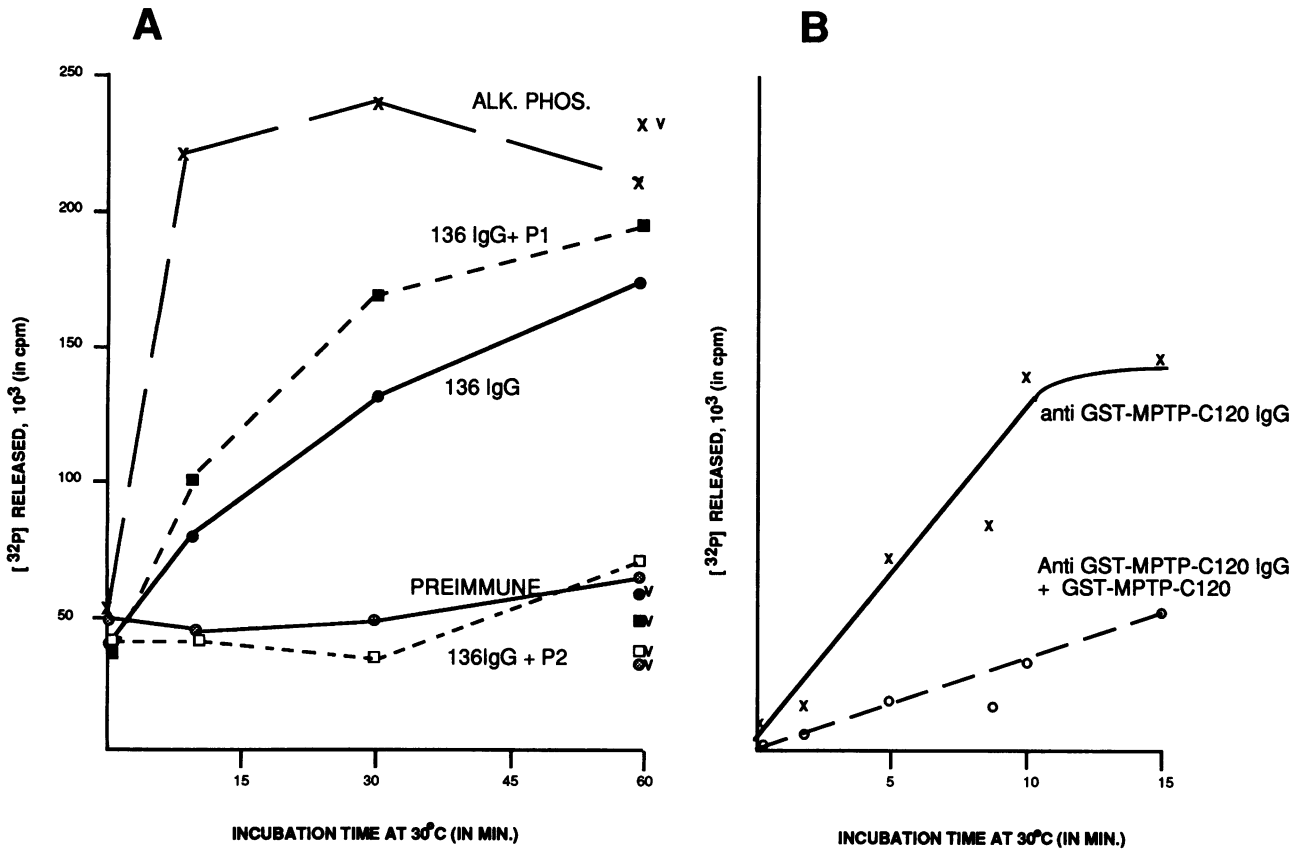

FIG. 4. Immunoprecipitation of the MPTP phosphatase activity. Kinetic analysis of ^{32}P-labeled Raytide dephosphorylation by various MPTP immunoprecipitates is shown. The same amount of labeled Raytide (6.50×10^5 cpm) was added to all immunoprecipitates in phosphatase buffer and incubated at 37°C. At appropriate time points, free [^{32}P]phosphate was estimated, and values were plotted accordingly. v indicates the addition of 1 mM sodium orthovanadate. (A) ×, alkaline phosphatase (ALK. PHOS.) assay; ●, immunoprecipitation with antiserum 136; ●, immunoprecipitation with preimmune antiserum 136; ■, immunoprecipitation with antiserum 136 in the presence of 100 ng of peptide P1; □, immunoprecipitation with antiserum 136 in the presence of 100 ng of peptide P2. (B) ×, immunoprecipitation with the anti-GST–MPTP-C120 fusion protein; ○, immunoprecipitation with anti-GST–MPTP-C120 fusion protein in the presence of GST–MPTP-C120 protein.

activity (V_{max}) of 44.4 μmol/mg of protein per min and a K_m of 0.476 mM.

In vivo activity of the MPTP. To identify the MPTP protein in vivo, we used both antiserum 136 and affinity-purified anti-GST–MPTP-C120 antibody to immunoprecipitate the MPTP protein from NIH 3T3 cells metabolically labeled with [^{35}S]methionine. However, we were unable to detect any MPTP polypeptide after fluorography of the SDS-polyacrylamide gel. Likewise, Western blot analysis of these cell lysates failed to detect the MPTP (data not shown). In view of the high in vitro activity of the enzyme and the demonstrated specificity of the antibodies used, we attributed our failure to detect the enzyme to the low abundance or the possible sequestering of the MPTP within the cells. Therefore, to enhance the sensitivity of detection, we chose to assay the immunoprecipitates for the presence of PTPase activity by using ^{32}P-labeled Raytide as a substrate. As shown in Fig. 4A, purified immunoglobulins from antiserum 136 precipitated PTPase activity that was absent when immunoglobulins from preimmune serum were used. Moreover, the cognate antigenic peptide P2 but not an unrelated peptide (P1) reduced PTPase activity in the immunocomplexes. The PTPase activity immunoprecipitated with antiserum 136 was sensitive to sodium vanadate, whereas an alkaline phosphatase control reaction was not affected by the inhibitor. Similar results were obtained with the anti-GST–MPTP-C120 IgG (Fig. 4B). In summary, these results indicate that the mature intracellular form of the MPTP exists in vivo and that it possesses an intact carboxyl terminus as well as PTPase activity.

Nuclear localization of the β-galactosidase–MPTP fusion proteins. To identify the subcellular location of the MPTP, we engineered the *lacZ* gene such that it would allow for gene fusions at the 3′ end of the gene. To safeguard against potential toxic effects caused by an unregulated phosphotyrosine phosphatase activity, only sequences downstream from the region encoding the conserved active domain were included in the fusion proteins. The gene fusion plasmids (Fig. 1B) were transfected by the calcium phosphate method into COS1 cells, and after 48 h, the cells were fixed and assayed for expression of β-galactosidase, using immunofluorescence staining with an anti-β-galactosidase antibody (18). Initially, we compared the staining pattern obtained after transfection of pCH110.1 and pCH110.1/MPTP-C120. As shown in Fig. 5C, expression of an unmodified β-galactosidase led to intense fluorescence staining in the cytoplasm of cells. By comparison, cells that expressed the β-galactosidase chimera tagged with the 120-amino-acid carboxyl terminus of the MPTP exhibited staining exclusively in the nuclei of transfected cells (Fig. 5E).

Having established that the last 120 amino acids of the

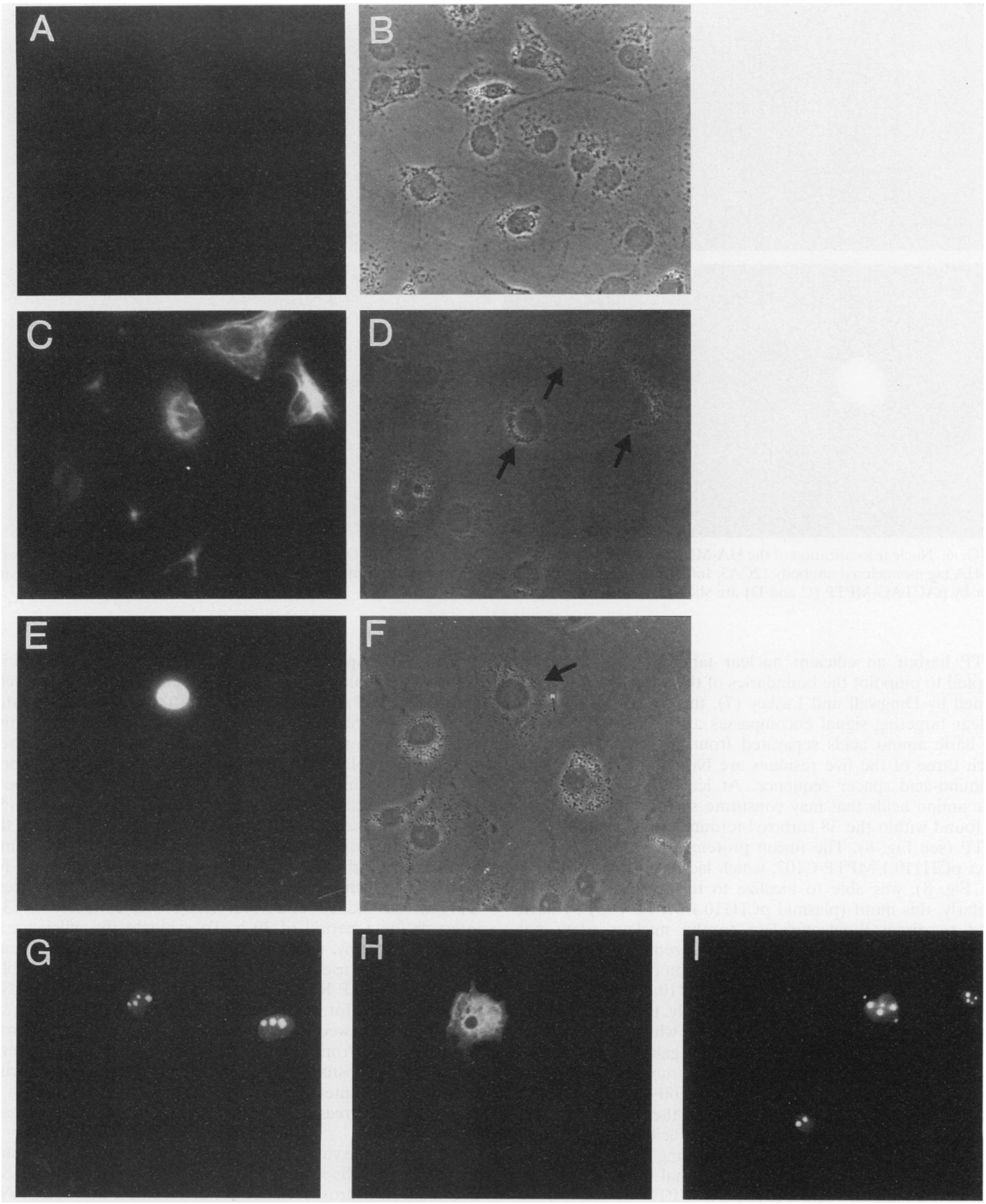

FIG. 5. Nuclear localization of the β-galactosidase–MPTP fusion protein. Shown are immunofluorescence staining and corresponding phase contrast of COS1 cells transfected with the following plasmids: pCH110.1 stained with an unrelated anti-factor IX monoclonal antibody (A and B), pCH110.1 stained with an anti-β-galactosidase monoclonal antibody (C and D), pCH110.1/MPTP-C120 stained with an anti-β-galactosidase monoclonal antibody (E and F), and pCH110.1/MPTP-C107 (G), pCH110.1/MPTP-C31 (H), and pCH110.1/MPTP-C38 (I) stained with an anti-β-galactosidase monoclonal antibody.

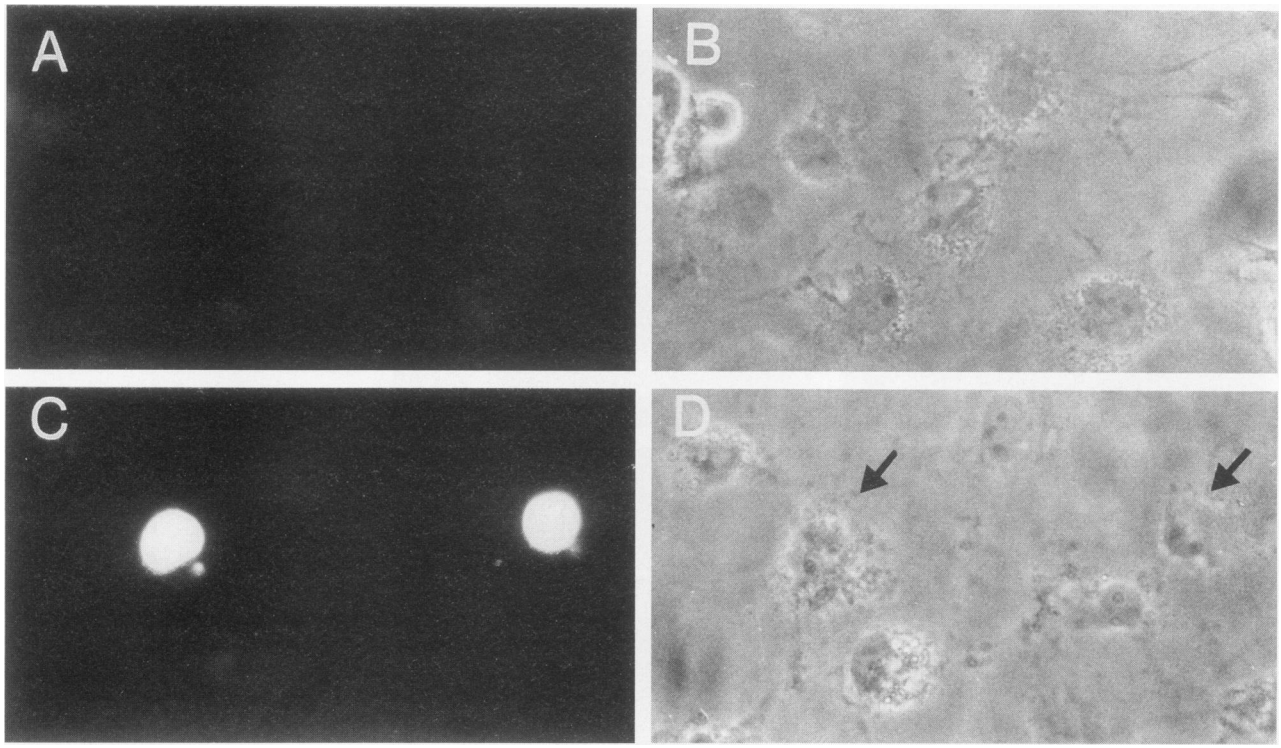

FIG. 6. Nuclear localization of the HA-MPTP fusion protein. At 24 h after transfection, COS1 cells were stained by immunofluorescence, using anti-HA tag monoclonal antibody 12CA5. Immunofluorescence and corresponding phase contrast of COS1 cells transfected by pACTAG (A and B) or by pACTAG-MPTP (C and D) are shown.

MPTP harbor an efficient nuclear targeting signal, we attempted to pinpoint the boundaries of this targeting motif. As defined by Dingwall and Laskey (7), the consensus bipartite nuclear targeting signal encompasses a first cluster made of two basic amino acids separated from a second cluster (in which three of the five residues are basic amino acids) by a 10-amino-acid spacer sequence. At least three stretches of basic amino acids that may constitute such a bipartite signal are found within the 38 carboxyl-terminal amino acids of the MPTP (see Fig. 8). The fusion protein expressed from construct pCH110.1/MPTP-C107, which lacks the basic cluster 3 (see Fig. 8), was able to localize to the nucleus (Fig. 5G). Similarly, this motif (plasmid pCH110.1/MPTP-C13) by itself failed to direct β-galactosidase to the nucleus (data not shown), indicating that cluster 3 was not required for nuclear localization. As shown in Fig. 5H, inclusion of cluster 2 in the fusion protein encoded by plasmid pCH110.1/MPTP-C31 did not restore nuclear targeting either. Finally, the fusion protein expressed from pCH110.1/MPTP-C38, which included all three clusters, was sufficient to direct β-galactosidase to the nucleus (Fig. 5I). Interestingly, some of our hybrid proteins appear to localize primarily in the nucleoli (Fig. 5G and I). Taken together, these results localize the MPTP nuclear localization signal (NLS) between amino acids 345 and 369.

To demonstrate that the nuclear targeting signal defined by the deletion analysis was actually functional in the MPTP, we generated a plasmid vector, pACTAG-MPTP, in which three influenza HA epitopes are linked in frame to the MPTP amino terminus (Fig. 1C). Following transfection into COS1 cells and immunostaining with monoclonal antibody 12CA5, no fluorescence was detected for the control plasmid pACTAG (Fig. 6A), and specific nucleus-localized fluorescence was seen with pACTAG-MPTP (Fig. 6C).

Cell cycle expression of the MPTP. Several observations suggest a possible role for the MPTP enzyme in the cell cycle: first, T-cell PTPase dephosphorylates the cell cycle-regulated *cdc2* kinase in vitro and complements a *cdc25* thermosensitive mutant at the nonpermissive temperature (12); second, expression of the T-cell PTPase homolog is ubiquitous, and overproduction of a truncated version of the T-cell PTPase has been shown to decrease the mitotic index of transfected cells (5); and third, as described above, the MPTP localizes to the nucleus. To further elucidate the regulation of this enzyme, we synchronized NIH 3T3 cell monolayers at low serum for 36 h, after which, at time zero, 15% fetal calf serum in fresh DMEM was added and total RNA was extracted at 3-h intervals for a period of 30 h. To evaluate the efficiency of cellular synchrony, tritiated thymidine incorporation for each time point was used as a control. The result of a slot blot analysis of MPTP RNA expression normalized to actin RNA levels is plotted for each corresponding time point in Fig. 7A. This analysis showed that MPTP RNA levels increased approximately 13-fold from a basic level found at G_0 to a high level peaking at 6 h postinduction, corresponding to late G_1. During S phase, represented by time points from 12 to 18 h, levels of MPTP RNA decreased rapidly, followed by a renewed increase in G_2.

To confirm the variation in MPTP RNA levels at late G_1 and G_2, NIH 3T3 cells were arrested in late G_1/S phase by an 8-h treatment in hydroxyurea. Cells were washed, and total RNA was isolated at 3-h intervals during a period of 12 h. At T_0, corresponding to late G_1 in the cell cycle, as with serum starvation, high levels of MPTP RNA were detected, followed by a significant reduction during S phase (T_6 to T_9) (Fig. 7B). Finally, at T_{12}, corresponding to early G_2, increasing amounts of MPTP RNA were also observed.

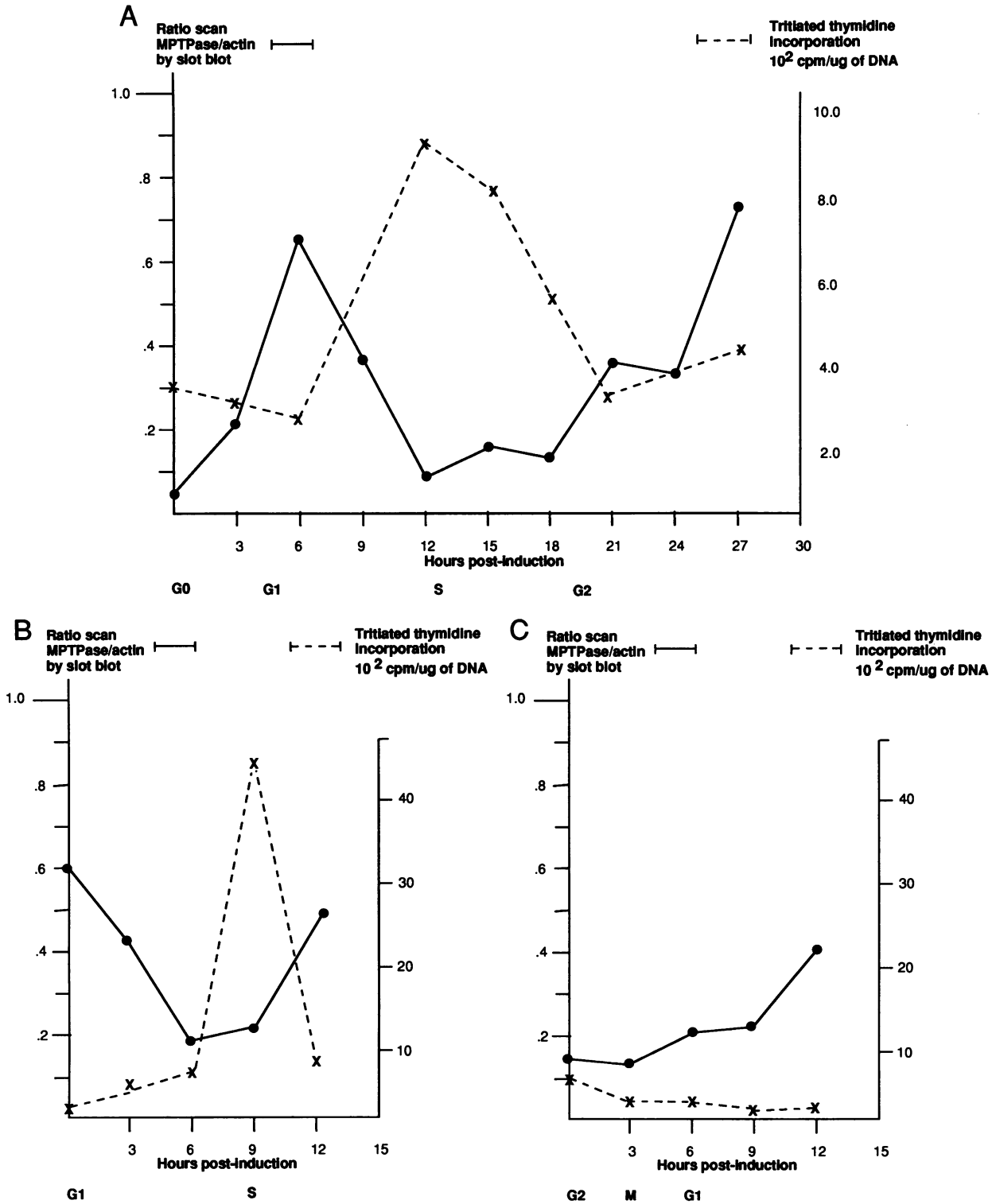

FIG. 7. Cell cycle regulation of the MPTP expression. Graphs represent the ratio of MPTP versus actin RNA level estimated by scanning densitometry of the autoradiograms. MPTP expression levels at various time points following cellular synchronization of NIH 3T3 cells by low serum (A), hydroxyurea (B), and nocodazole (C) are shown. ——, normalized level of MPTP RNA; – – –, tritiated thymidine incorporation.

The increase in MPTP RNA level at G_2 was further evaluated by synchronizing NIH 3T3 cells for 12 h with nocodazole, which blocks cells at late G_2. Efficiency of cell synchrony was monitored by tritiated thymidine incorporation and by changes in cellular morphology which are easily identifiable at the G_2/M junction. At T_0, fresh medium was added, and the cells were harvested at 3-h intervals for RNA isolation. At T_0 to T_3, corresponding to late G_2 and M, respectively, low

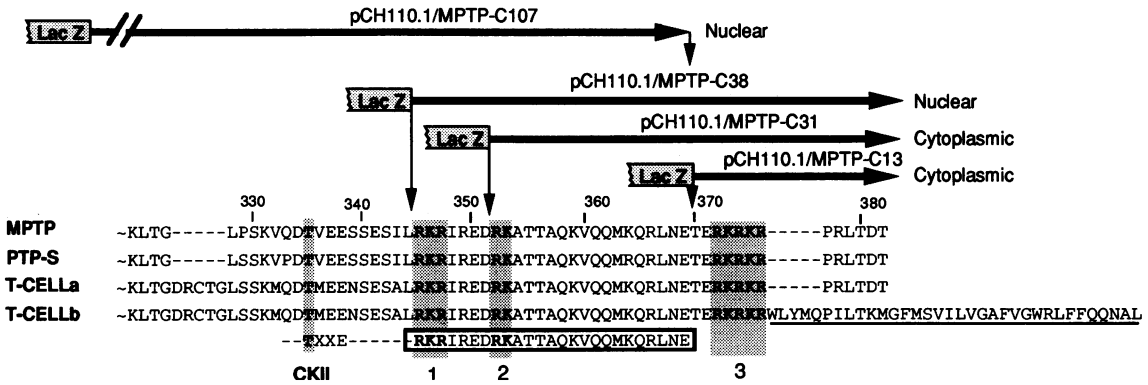

FIG. 8. Amino acid comparison of the carboxyl termini of the mouse (MPTP), rat (PTP-S), and human (T-cell PTPa [T-CELLa] and T-cell PTPb [T-CELLb]) PTPases. The putative casein kinase II (CKII) phosphorylation site and the three basic amino acid clusters are indicated in boldface inside the shaded areas. Thick arrows indicate the LacZ fusion proteins used in the identification of the MPTP NLS. The minimal 25-amino-acid domain (amino acids 345 to 369) identified as containing the MPTP NLS is shown in the boxed area.

levels of MPTP RNA are detected in nocodazole-synchronized cells, followed thereafter by a constant increase in RNA levels from T_6 to T_{12} (Fig. 7C).

DISCUSSION

In this study, we have shown that the full-length bacterially produced MPTP can dephosphorylate pNPP with high efficiency. The MPTP exhibited a 10- to 100-fold-higher affinity than other phosphatases assayed under the same conditions. For example, a K_m of 50 mM was reported for cdc25 (8, 11), compared with 0.476 mM for the MPTP. Like activities of other PTPases, MPTP activity was very sensitive to vanadate and $ZnCl_2$ (34). Unlike the T-cell PTPb, MPTP did not seem to require proteolytic processing at the carboxyl terminus to acquire enzymatic activity, since a specific antipeptide serum directed against the last 10 carboxyl-terminal amino acids recognized this sequence in the enzymatically active bacterial protein and was able to immunoprecipitate functional enzyme from cells in vivo. Although we can immunoprecipitate the HA-tagged MPTP protein produced in transiently transfected COS1 cells with both the 136 IgG and the anti-C-120 IgG sera (data not shown), we failed to identify the endogenous MPTP from metabolically labeled cells. In addition to the low affinity of these antisera, the high specific activity of this enzyme suggests that cells may contain only minute amounts of MPTP. Sequestration of the enzyme in the nucleus, perhaps in combination with a restricted period of expression during the cell cycle, may have further impeded its release during extract preparation.

To date, several studies have addressed the subcellular localization of the nonreceptor PTPases. The nature of the subcellular localization of the T-cell PTPb has yet to be clarified. However, both rat PTPase 1 and the human placental PTPase 1B are targeted to the endoplasmic reticulum (10, 37). The presence of a nuclear targeting signal in all human and rodent T-cell PTPase homologs suggests that these enzymes constitute a unique group of PTPases. Our results show that the region encompassing the 38-amino-acid carboxyl terminus of the MPTP can specifically localize a β-galactosidase chimeric protein to the nucleus of transfected cells. Furthermore, nuclear localization was also found with the full-length MPTP protein linked to the HA tag. The failure of mutant p110.1/MPTP-C31 to localize to the nucleus suggests that the basic cluster I (RKR, amino acids 345 to 347) is an essential component of the NLS. On the contrary, nuclear localization of the fusion protein p110.1/MPTP-C107 shows that the basic motif III is not a component of the targeting motif. Thus, the NLS does not conform to the consensus bipartite sequence proposed by Dingwall and Laskey (7), since no basic cluster separated by the consensus 10-amino-acid spacer region exists in the carboxyl-terminal region between amino acids 345 and 369. The results of these experiments indicate that the MPTP NLS resembles the NLS motifs present in simian virus 40 large T antigen (7, 29) and in the nucleolus-localized human immunodeficiency virus Tat protein (30).

In addition to the nuclear signal, we have identified a casein kinase II site located in proximity to the NLS (Fig. 8). Phosphorylation of the threonine residue contained within this site might modulate the rate of nuclear transport as described by Rihs et al. (23, 24).

Nuclear localization of MPTP would expose the enzyme to a unique set of potential substrates, notably nuclear targets that may play a role in regulating the cell cycle. The analysis of MPTP RNA steady-state levels showed low levels in G_0. However, our data revealed that high levels of MPTP RNA are consistently present at late G_1 with the three synchronization methods used. The increase in G_2 seen with serum starvation and hydroxyurea is absent in nocodazole-treated cells (Fig. 7). This discrepancy may result from cellular desynchrony in S phase. This fact would also explain the increase in tritiated thymidine incorporation visible at T_{27} in serum starved cells (Fig. 7A).

At least three classes of genes have been shown to be induced in G_1: the immediate-early genes that are rapidly induced (e.g., c-*fos*), the delayed-response genes that require several hours to appear (e.g., HMGI-C), and the S-phase genes induced in late G_1 that are required for DNA replication (e.g., the thymidine kinase and thymidylate synthetase genes) (14, 16). Our results would place the MPTP in the latter category.

Phosphorylation of proteins on tyrosine is a pivotal mechanism for the regulation of protein function in eukaryotic cells. Therefore, it is likely that the enzymes which are instrumental for exerting this control are themselves tightly controlled with regard to their production and activity. Our results have demonstrated two possible ways to regulate the MPTP. First, localization of this enzyme in the nucleus would limit accessibility of the MPTP to nuclear substrates. Second, MPTP mRNA is expressed to a higher degree at a specific time during the cell cycle, further restricting potential substrates to a certain stage of the cell cycle. It is important to note, however,

that the level of MPTP protein expression and of its enzymatic activity may not follow the RNA level profile. We have so far failed in quantitating MPTP enzymatic activity throughout the cell cycle.

In the case of T-cell PTPa and -b, alternative splicing gives rise to two different carboxyl termini (2) that may dictate two different subcellular localizations of the enzymes. Given the extensive homology between the MPTP and both forms of the T-cell PTPase, which includes the nuclear targeting signal, it would appear that the addition of the hydrophobic domain in the T-cell PTPb sets the switch for overriding nuclear localization and directing the enzyme to high-molecular-weight complexes. Recently, McLaughlin and Dixon (19) reported the existence of a novel intracellular PTPase, dPTP61F, that can either localize to the nucleus or remain cytoplasmic, depending on the carboxyl-terminal sequence generated by differential splicing.

The recent identification of several tyrosine-phosphorylated proteins in the nucleus, such as the transcription factors p91 (25, 28), SIF A (26), and interleukin-4 NAF (15), emphasizes the critical importance of MPTP nuclear localization. Even though the function of the MPTP is still unknown, two possible mechanisms of action may be proposed. The MPTP could recognize specific substrates, allowing a particular one to be recycled, or alternatively, this enzyme could operate as a scavenger for all available nuclear tyrosine-phosphorylated proteins, perhaps at a particular cell cycle stage. Our observation that the MPTP is present in the nucleus and that its mRNA level is elevated in late G_1 may help in identifying candidate substrates and thus clarify which one of these mechanisms is more likely.

ACKNOWLEDGMENTS

We are grateful to Flavio Lejbkowicz for assistance in the immunofluorescence studies, Alain Charest for the pACTAG vector, Yaron Nophar for help with the illustrations, and André Veillette and Philip E. Branton for critical reading of the manuscript. We also thank Nahum Sonenberg for helpful discussions.

This work was supported in part by the National Cancer Institute of Canada (M.L.T.). D.B. is a recipient of a studentship from the Fonds pour la Formation de Chercheurs et l'Aide à la Recherche. M.L.T. is a Fraser, Monat and McPherson Scholarship recipient.

REFERENCES

1. **Alphey, A., J. Jimenez, H. White-Cooper, I. Dawson, P. Nurse, and D. M. Glover.** 1992. Twine, a cdc25 homolog that functions in the male and female germline of Drosophila. Cell **69:**979–988.

1a. **Bradford, M. M.** 1976. A rapid and sensitive method for the quantitation of microgram quantities of protein utilizing the principle of protein-dye binding. Anal. Biochem. **72:**248–254.

2. **Champion-Arnaud, P., M. C. Gesnel, N. Foulkes, C. Ronsin, P. Sassone-Corsi, and R. Breathnach.** 1991. Activation of transcription via AP-1 or CREB regulatory sites is blocked by protein tyrosine phosphatases. Oncogene **6:**1203–1209.

3. **Church, G. M., and W. Gilbert.** 1984. Genomic sequencing. Proc. Natl. Acad. Sci. USA **81:**1991–1995.

4. **Cool, D. E., P. R. Andreassen, N. K. Tonks, E. G. Krebs, E. H. Fischer, and R. L. Margolis.** 1992. Cytokinetic failure and asynchronous nuclear division in BHK cells overexpressing a truncated protein-tyrosine-phosphatase. Proc. Natl. Acad. Sci. USA **89:** 5422–5426.

5. **Cool, D. E., N. K. Tonks, H. Charbonneau, E. H. Fischer, and G. Krebs.** 1990. Expression of a human T-cell protein-tyrosine-phosphatase in baby hamster kidney cells. Proc. Natl. Acad. Sci. USA **87:**7280–7284.

6. **Cool, D. E., N. K. Tonks, H. Charbonneau, K. A. Walsh, E. H. Fischer, and E. G. Krebs.** 1989. cDNA isolated from a human T-cell library encodes a member of the protein-tyrosine-phosphatase family. Proc. Natl. Acad. Sci. USA **86:**5257–5261.

7. **Dingwall, C., and R. A. Laskey.** 1991. Nuclear targeting sequences—a consensus? Trends Biochem. Sci. **16:**478–481.

8. **Dunphy, W. G., and A. Kumagai.** 1991. The cdc25 protein contains an intrinsic phosphatase activity. Cell **67:**189–196.

9. **Fischer, E. H., H. Charbonneau, and N. K. Tonks.** 1991. Protein tyrosine phosphatases: a diverse family of intracellular and transmembrane enzymes. Science **253:**401–406.

10. **Frangioni, J. V., P. H. Beahm, V. Shifrin, C. A. Jost, and B. G. Neel.** 1992. The nontransmembrane tyrosine phosphatase PTP-1B localizes to the endoplasmic reticulum via its 35 amino acid C-terminal sequence. Cell **68:**545–560.

11. **Gautier, J., M. J. Solomon, R. N. Booher, J. F. Bazan, and M. W. Kirschner.** 1991. cdc25 is a specific tyrosine phosphatase that directly activates $p34^{cdc2}$. Cell **67:**197–211.

12. **Gould, K. L., S. Moreno, N. K. Tonks, and P. Nurse.** 1990. Complementation of the mitotic activator, $p50^{cdc25}$ by a human protein-tyrosine phosphatase. Science **250:**1573–1576.

13. **Graham, F. L., and A. J. van der Eb.** 1973. A new technique for the assay of infectivity of human adenovirus 5 DNA. Virology **52:**456–465.

14. **Johnson, L. F.** 1992. G1 events and the regulation of genes for S-phase enzymes. Curr. Opin. Cell Biol. **4:**149–154.

15. **Kotanides, H., and N. C. Reich.** 1993. Requirement of tyrosine phosphorylation for rapid activation of a DNA binding factor by IL-4. Science **262:**1265–1267.

16. **Lanahan, A., J. B. Williams, L. K. Sanders, and D. Nathans.** 1992. Growth factor-induced delayed early response genes. Mol. Cell. Biol. **12:**3919–3929.

17. **Lejbkowicz, F., C. Goyer, A. Darveau, S. Neron, R. Lemieux, and N. Sonenberg.** 1992. A fraction of the mRNA 5′ cap-binding protein, eukaryotic initiation factor 4E, localizes to the nucleus. Proc. Natl. Acad. Sci. USA **89:**9612–9616.

18. **Manrow, R. E., A. R. Sburlati, J. A. Hanover, and S. L. Berger.** 1991. Nuclear targeting of prothymosin alpha. J. Biol. Chem. **266:**3916–3924.

19. **McLaughlin, S., and J. E. Dixon.** 1993. Alternative splicing gives rise to a nuclear protein tyrosine phosphatase in Drosophila. J. Biol. Chem. **268:**6839–6842.

20. **Mosinger, B., Jr., U. Tillmann, H. Westphal, and M. L. Tremblay.** 1992. Cloning and characterization of a mouse cDNA encoding a cytoplasmic protein-tyrosine-phosphatase. Proc. Natl. Acad. Sci. USA **89:**499–503.

21. **Niman, H. L., R. A. Houghten, L. E. Walker, R. A. Reisfeld, I. A. Wilson, J. M. Hogle, and R. A. Lerner.** 1983. Generation of protein-reactive antibodies by short peptides is an event of high frequency: implications for the structural basis of immune recognition. Proc. Natl. Acad. Sci. USA **80:**4949–4953.

22. **Perkins, L. A., I. Larsen, and N. Perrimon.** 1992. *corkscrew* encodes a putative protein tyrosine phosphatase that functions to transduce the terminal signal from the receptor tyrosine *torso*. Cell **70:**225–236.

23. **Rihs, H. P., D. A. Jans, H. Fan, and R. Peters.** 1991. The rate of nuclear cytoplasmic protein transport is determined by the casein kinase II site flanking the nuclear localization sequence of the SV-40 T-antigen. EMBO J. **10:**633–639.

24. **Rihs, H. P., and R. Peters.** 1989. Nuclear transport kinetics depend on phosphorylation-site-containing sequences flanking the karyophilic signal of the simian virus T-antigen. EMBO J. **8:**1479–1484.

25. **Ruff-Jamison, S., K. Chen, and S. Cohen.** 1993. Induction by EGF and interferon-γ of tyrosine phosphorylated DNA binding proteins in mouse liver nuclei. Science **261:**1733–1736.

26. **Sadowski, H. B., K. Shuai, J. E. Darnell, Jr., and M. Z. Gilman.** 1993. A common nuclear signal transduction pathway activated by growth factor and cytokine receptors. Science **261:**1739–1744.

27. **Shen, S.-H., L. Bastien, B. I. Posner, and P. Chretien.** 1991. A protein-tyrosine phosphatase with sequence similarity to the SH2 domain of the protein-kinases. Nature (London) **352:**736–739.

28. **Shuai, K., G. R. Stark, I. M. Kerr, and J. E. Darnell, Jr.** 1993. A single phosphotyrosine residue of Stat91 required for gene activation by interferon-γ. Science **261:**1744–1746.

29. **Silver, P. A.** 1991. How proteins enter the nucleus. Cell **64:**489–497.

30. **Siomi, H., H. Shida, M. Maki, and M. Hatanaka.** 1990. Effects of

a highly basic region of human immunodeficiency virus Tat protein on nucleolar localization. J. Virol. **64:**1803–1807.

31. **Smith, D. B., and K. S. Johnson.** 1988. Single-step purification of polypeptides expressed in *Escherichia coli* as fusions with glutathione S-transferase. Gene **67:**31–40.
32. **Streuli, M., N. X. Krueger, A. Y. W. Tsai, and H. Saito.** 1990. Distinct functional roles of the two intracellular phosphatase like domains of receptor-linked protein tyrosine phosphatases LCA and LAR. EMBO J. **9:**2399–2407.
33. **Swarup, G., S. Katmatkar, V. Radha, and V. Rema.** 1991. Molecular cloning and expression of a protein-tyrosine phosphatase showing homology with transcription factors Fos and Jun. FEBS Lett. **280:**65–69.
34. **Tonks, N. K., C. D. Diltz, and E. H. Fischer.** 1988. Characterization of the major protein-tyrosine-phosphatases of human placenta. J. Biol. Chem. **263:**6731–6737.
35. **Woodford-Thomas, T. A., J. D. Rhodes, and J. E. Dixon.** 1992. Expression of a protein tyrosine phosphatase in normal and *v-src*-transformed mouse 3T3 fibroblasts. J. Cell Biol. **117:**401–404.
36. **Zander, N. F., D. E. Cool, C. D. Diltz, L. R. Rohrschneider, E. G. Krebs, and E. H. Fischer.** 1993. Suppression of v-fms-induced transformation by overexpression of a truncated T-cell protein tyrosine phosphatase. Oncogene **8:**1175–1182.
37. **Zander, N. F., J. A. Lorenzen, D. E. Cool, N. K. Tonks, G. Daum, E. G. Krebs, and E. H. Fischer.** 1991. Purification and characterization of a human recombinant T-cell protein-tyrosine-phosphatase from a baculovirus expression system. Biochemistry **30:** 6964–6970.